LA-UR-15-27993
Approved for public release; distribution is unlimited.

Title:	Characterization and corrosion behavior test of glass ceramic waste form
Author(s):	Tang, Ming
Intended for:	Report
Issued:	2015-10-14

Characterization and corrosion behavior test of glass ceramic waste form

Fuel Cycle Research & Development

Prepared for
U.S. Department of Energy
Material Recovery & Waste Form Development Campaign

Ming Tang
Los Alamos National Laboratory

September 10, 2015

FCRD-MRWFD-2015-000340

Name/Title of Deliverable/Milestone	Characterization and corrosion behavior test of glass ceramic waste form **M3FT-15LA0307031**
Work Package Title and Number	Glass Ceramic-LANL **FT-15LA030703**
Work Package WBS Number	**1.02.03.07**
Responsible Work Package Manager	Ming Tang *(Name/Signature)*
Date Submitted	*09/10/2015*

Quality Rigor Level for Deliverable/Milestone

☒ *Rigor Level 3* ☐ *Rigor Level 2* ☐ *Rigor Level 1* ☐ *Nuclear Data*

This deliverable was prepared in accordance with *Ming Tang* *(Participant's Name)*

QA program which meets the requirements of

☐ *DOE Order 414.1* ☐ *NQA-1-2000*

This Deliverable was subjected to:

☒ *Independent Technical Review* ☐ *Peer Review*

Independent Technical Review (ITR)

Review Documentation Provided

☐ *Signed ITR Report or,*

☐ *Signed ITR Concurrence Sheet or,*

☒ *Signature of ITR Reviewer(s) below*

Peer Review (PR)

Review Documentation Provided

☐ *Signed PR Report or,*

☐ *Signed PR Concurrence Sheet or,*

☐ *Signature of PR Reviewer(s) below*

Name and Signature of Peer Reviewers(s)/Independent Technical Reviewer(s)

Osman Anderoglu

SUMMARY

The research conducted in this work package is to collect data in support of future development of glass ceramic waste forms and to help develop the next generation high performance waste management technologies. This work package collaborates closely with the work conducted under “Glass Ceramic – Pacific Northwest National Laboratory (PNNL) - (FT-15PN030704)” and “CCIM Test with Glass Ceramic – Idaho National Laboratory (INL) – (FT-15IN030707)”.

The Los Alamos National Laboratory (LANL) is focusing on characterization, testing procedures on glass ceramics from the test matrix and melter testing to further develop and mature the glass ceramic waste form for immobilization of high level waste (HLW) raffinate stream. In Fiscal Year 2015, we are mainly working on multi-phase glass ceramic waste forms. Various characterization and testing techniques (including X-ray diffraction, transmission electron microscopy/scanning transmission electron microscopy, scanning electron microscopy, synchrotron X-ray, nano-indentation) were used to characterize and investigate the corrosion behavior of glass ceramics.

CONTENTS

FIGURES

1. Electron microscopy characterizations and nano-indentation tests on corrosion behavior of glass ceramics

Borosilicate glass-ceramics containing oxyapatite and powellite crystals are being developed to immobilize high-level waste fission products into a stable waste form after they have been separated from used nuclear fuel by aqueous reprocessing. The corrosion behavior of this multi-phase waste form is expected to be complex due to the unique corrosion rates of each individual phase, the grain boundaries, and the interaction layers between phases. To begin a detailed investigation of the corrosion behavior of this multi-phase waste form, a modified single-pass flow-through test (SPFT) was selected to study polished monolithic coupons at pH (25 °C) value of 7 and 90 °C for 33 days in dilute solution conditions at PNNL. The altered coupons were examined with scanning electron microscopy (SEM), transmission electron microscopy/scanning transmission electron microscopy (TEM/STEM), and nano-indentation tests to study the corrosion behavior of the bulk waste form and the individual phases, as well as to examine the crystal-glass interface.

1.1 SEM characterization on SPFT glass ceramics

SEM characterization on two SPFT glass ceramic waste form samples C1-2013 and 010-CCC were performed at electron microscopy lab (EML), LANL, using FEI Inspect F SEM outfitted with energy dispersive x-ray spectroscopy (EDX). SPFT samples was face-to-face glued with a silicon wafer as a control, then polished in cross-section geometry with alumina lapping films to obtain a mirror finish for SEM observation. All of these samples were final polished with 40 nm colloidal silica slurry (Syton HT50, DuPont AirProducts NanoMaterials L.L.C, Tempe, AZ), in order to remove the surface damage created by mechanical polish.

Figure 1 shows cross-sectional SEM images of C1-2013 (a) and 010-CCC (b) samples. Based on SEM/EDX observation, the C1-2013 sample had an altered glass layer (~300 nm in thickness) formed between crystal and glass, and Na was found to be depleted (EDX not shown here). However, no altered glass layer was found in 010-CCC sample in cross-section.

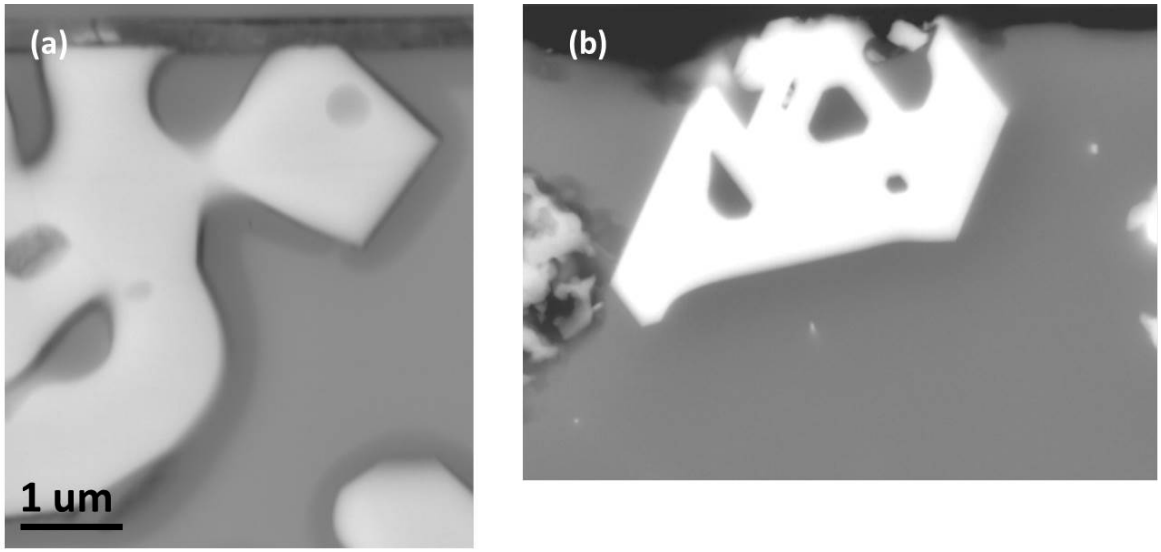

Figure 1. Cross-sectional SEM images of C1-2013 (a) and 010-CCC (b) samples.

1.2 TEM/STEM characterization on SPFT glass ceramics

Alternation layers are a common feature of leached surfaces of borosilicate waste glasses [1-5]. Figure 2 shows schematic representation of HLW glass corrosion with progressive formation of an alteration layer and ultimately amorphous and crystalline secondary phases [6]. Detailed knowledge of the mechanism controlling chemical alteration is fundamental for predicting the long term radionuclide retention potential of nuclear borosilicate glasses in contact with aqueous fluids in geologic repositories. In this work, we applied a unique combination of TEM/STEM techniques with very high spatial and mass resolution to obtain high resolution structural images, and two- and three-dimensional chemical distribution maps of the glass-altered zone interfacial region.

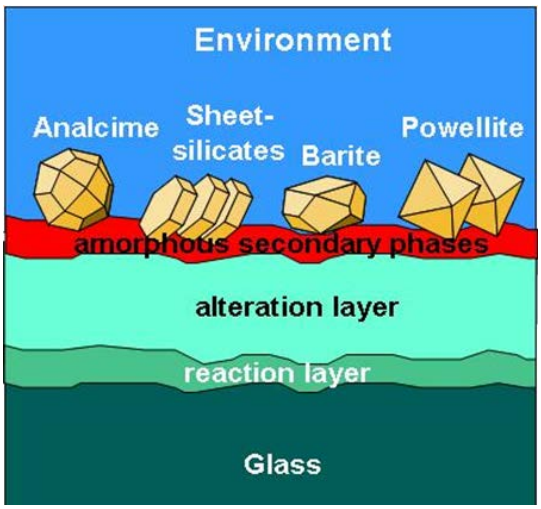

Figure 2. Schematic representation of HLW glass corrosion with progressive formation of an alteration layer and ultimately amorphous and crystalline secondary phases [6].

TEM/STEM characterizations on SPFT glass ceramic waste form sample C1-2013 were performed at EML, LANL, using FEI Tecnai F30 analytical TEM and FEI Titan 80-300 monochromated, image aberration-corrected imaging, and analytical TEM with full EDS and EELS imaging and analysis, which include sub-Å TEM, 1.4 Å STEM, TEM and STEM tomography, and Lorentz imaging. Samples were prepared in cross-sectional geometries for TEM/STEM examination, and the final thinning process to electron transparent was done with ion milling using Gatan Precision ion polishing system (PIPS).

Figure 3 shows TEM observation of crystal-glass interface in C1-2013 sample. Low magnification TEM bright field image (left) allows us to discriminate the altered layer from the glass and crystalline phase. The observed width of the altered layer is ~ 300 nm. The altered layer consists of two sub-layers (dark and bright sub-layers), and each layer has homogeneous morphology and structure. Intermediate magnification image (middle), shows that the bright sub-layer (also called as interfacial phase) between crystalline phase and dark altered layer is ~ 50 nm in width, and both bright and dark sub-layers are amorphous phase which is similar to glass.

High resolution TEM image (right) shows sharp interface between amorphous and crystalline phase.

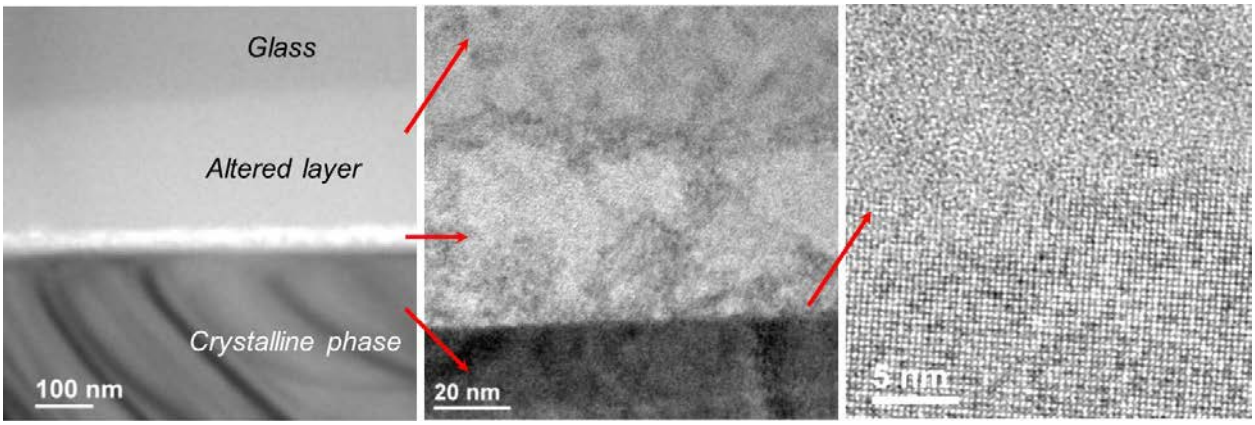

Figure 3. TEM observation of crystal-glass interface in C1-2013 sample.

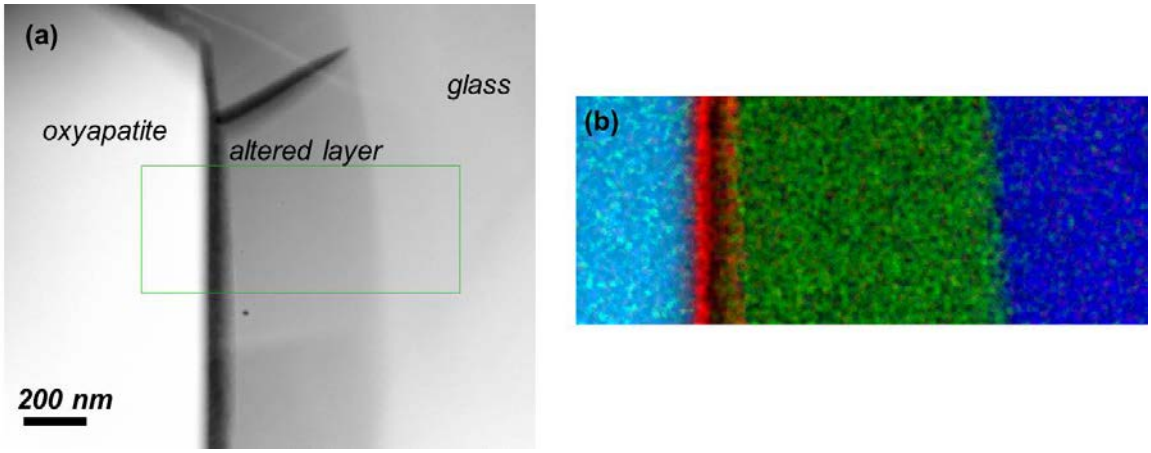

Figure 4. STEM image with HAADF detector of oxyapatite-glass interface.

Figure 4 shows STEM image with high-angle annular dark-field (HAADF) detector of oxyapatite-glass interface. Consistent with TEM observation, STEM image (Fig. 4(a)) reveals four regions with different Z contrast, which include oxyapatite (left), bright glass (right), dark glass, interfacial phase between oxyapatite and dark glass. The altered layer includes dark glass (heavily hydrated glass) and interfacial phase. The interfaces between these four regions are always distinct and very sharp. The different contrast in STEM observation means different

chemical composition, brighter contrast suggests heavier mass, and dark contrast is light mass. Using EDX elemental mapping, we qualitatively mapped the two-dimensional chemistry of the green rectangle area in Fig. 4(a) including oxyapatite, interfacial phase, dark glass, bright glass, at nanometer resolution. EDX mapping result in Fig. 4(b) shows clear difference in the composition among these four phases, and altered layer including interfacial and dark glass is chemically different from the pristine bright glass. Different colors in this mapping represent different phases, light blue for oxyapatite, red for interfacial phase, green for dark glass, dark blue for bright pristine glass. Figure 5 shows EDX spectrum of these four phases. Based on the spectrum, rich Carbon and higher Al/Si ratio are observed in interfacial phase, and Na is almost disappear in both interfacial phase and dark glass phase. EDX observation indicates that Na and Ca are almost depleted in altered layer, Si, Al, and Zr remained; and Si is partially depleted in the interfacial phase.

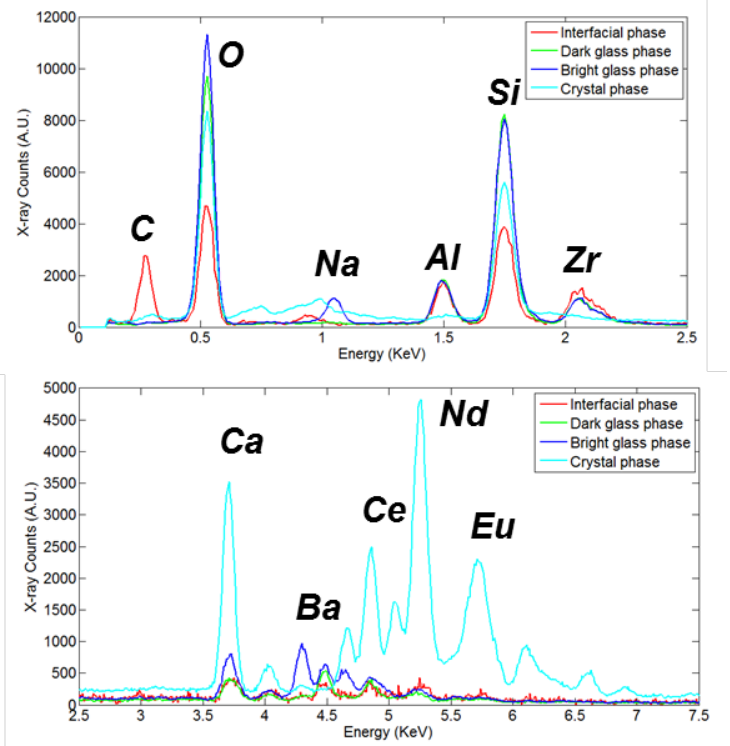

Figure 5. EDX spectrum of altered layer.

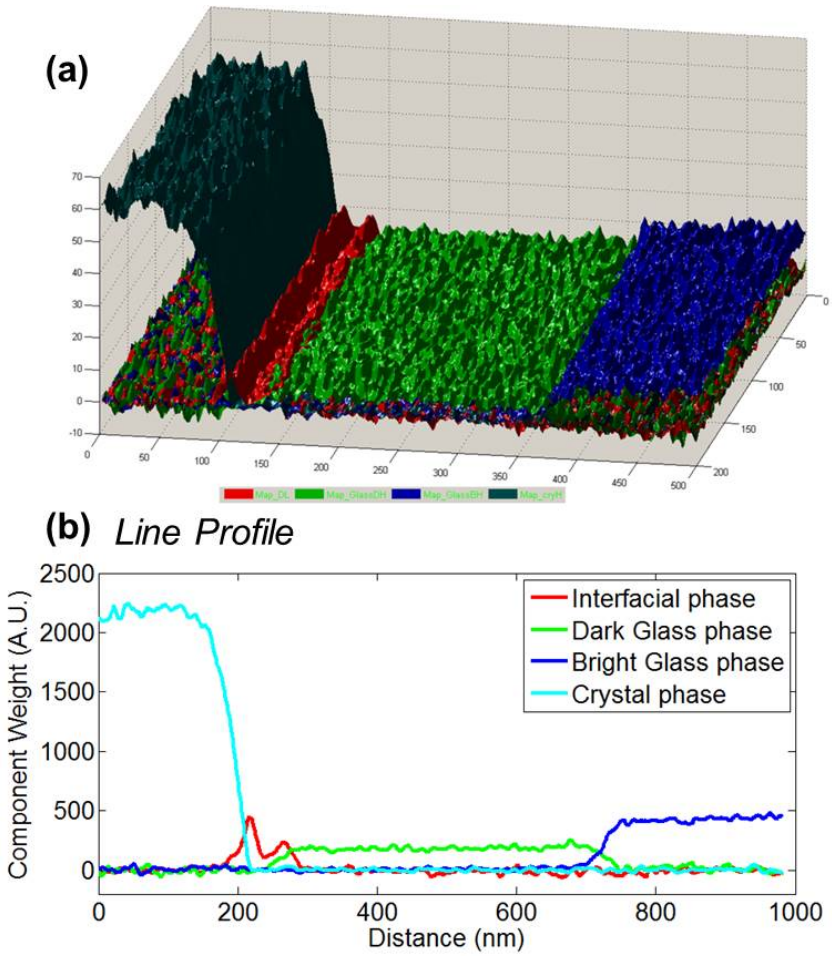

Figure 6. Three-dimensional reconstruction (a) and line profile (b) of EDX mapping.

Figure 6 shows a three-dimensional reconstruction (a) and line profile (b) of EDX mapping. The three-dimensional EDX reconstruction confirms that there are four chemically distinct regions in observed area, and the atomically sharp chemical interface separating these regions is very apparent. EDX line profile also reveals that crystalline phase has the highest component weight, and the altered layer has lower component weight than the pristine glass which suggests some elements are depleted in the altered layer. This observation is good agreement with the TEM/STEM results.

The mechanism controlling glass alteration in aqueous fluids has been controversial. In the past, two models prevailed [7]: one advocated that a hydrated and cation-depleted altered surface zone forms by an in situ transformation process controlled by diffusion and selective cation exchange; the other model postulated that precipitation of dissolved constituents form the glass results in a surface layer of secondary crystalline phase. To explore a universal reaction mechanism that controls glass corrosion, we need more detail experimental investigation and theoretical calculation to support and provide evidence. In the future, we will continue to employ advanced analytical characterization techniques like energy filtered TEM (EFTEM), electron energy-loss spectroscopy (EELS) in this study, to reveal more detail structural and chemical information of alteration zone.

1.3 Nano-indentation test on SPFT glass ceramics

Not only chemical and structural evolution, but also mechanical properties evolution, could be induced in glass ceramic waste forms under corrosion test. To investigate the mechanical properties evolution and understand the corrosion behavior of multi-phase glass ceramic waste forms, cross-section nano-indentation tests were performed on SPFT glass ceramics. Young's modulus and hardness data corresponding to different crystal/glass phases and corroded/uncorroded areas, suggests that mechanical properties changes could affect the overall performance of chemical durability.

SPFT sample C1-2013 was face-to-face glued with a silicon wafer as a control, then polished in cross-section geometry with alumina lapping films to obtain a mirror finish. All of these samples were final polished with 40 nm colloidal silica slurry (Syton HT50, DuPont AirProducts NanoMaterials L.L.C, Tempe, AZ), in order to remove the surface damage created by mechanical polish. This process provided a very flat and smooth surface as required for cross-

sectional nano-indentation. The nano indenter used was a Hysitron Triboindenter instrument equipped with a multi-range nanoprobe, an optical microscope and an atomic force microscope (AFM). A Berkovich diamond indenter tip was used to perform the nano-indentation measurements. Totally 75 indents were performed at various areas in glass ceramic samples. The indents were 5 μm apart from each other, and approximately 500 nm deep, so they should be about 2-3 μm wide. Constant displacement mode was used for all indents to ensure constant indentation depth.

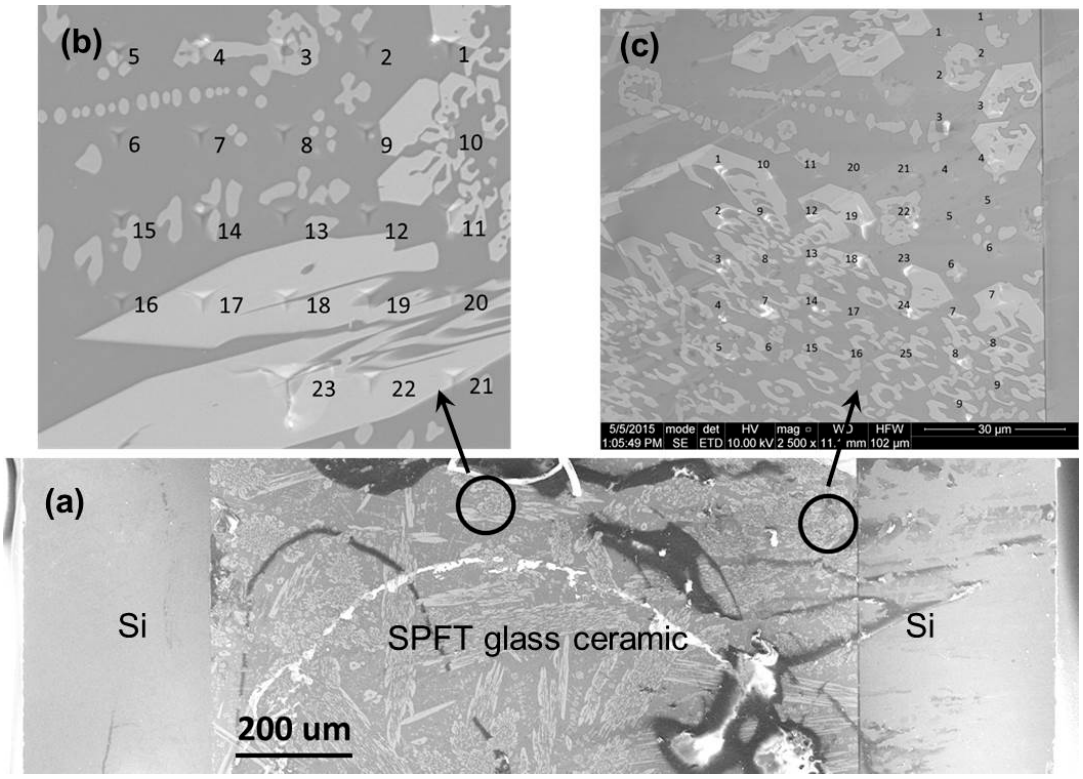

Figure 7. SEM images of nano indents in cross-sectional SPFT glass ceramic sample.

Figure 7 shows SEM images of nano indents in cross-sectional SPFT glass ceramic sample. In low magnification SEM image (Fig. 7(a)), there are three components of this cross-sectional sample, including Si, SPFT glass ceramic, and Si. The corroded area starts from the Si-glass ceramic interface to 30-40 μm deep area in SPFT glass ceramic sample. We performed nano-

indentation in two areas: one (Fig. 7(b)) is far from Si-glass ceramic interface (~ 500 um), another is from interface to 50 um depth (Fig. 7(c)). In Fig. 1(a) and (b), the indents are clearly observable, and some indents were performed on glass matrix, some on crystalline phases. Composition of crystalline phase is determined by EDX analysis.

To investigate mechanical properties evolution due to corrosion, Young's modulus and hardness in the same phase are compared as a function of distance from surface. Figure 8 shows the comparisons on glass phase (left) and oxyapatite phase (right). In this test, the area between surface to 30-40 um deep is considered as corroded by SPFT, and the area in 500 um deep is uncorroded. In both phases, Young's modulus and hardness show the same trend: the closer to surface, the softer in hardness and lower in modulus. This evolution could be due to the chemistry and structural changes as a result of corrosion. This comparison suggests that corrosion affects the mechanical properties evolution in glass ceramic because the area close to surface is severely corroded.

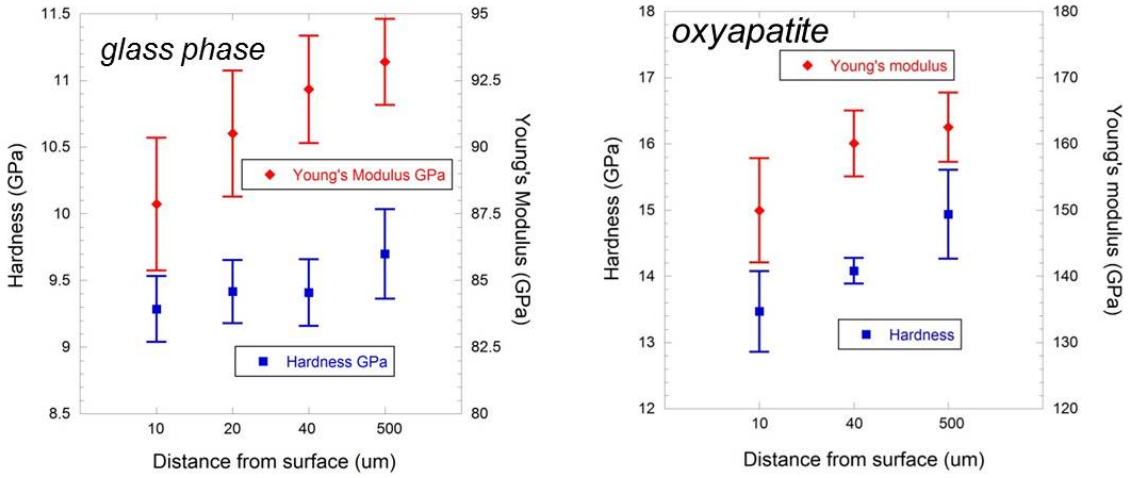

Figure 8. Mechanical properties evolution of SPFT glass ceramic as a function of distance from surface.

Young's modulus and hardness of different phases in the same area are also compared. Figure 9(a) shows SEM observation of the area close to Si/glass ceramic interface which is at the right

side of image. Some indents are on glass, one on oxyapatite, one on the altered layer at the glass-oxyapatite interface.

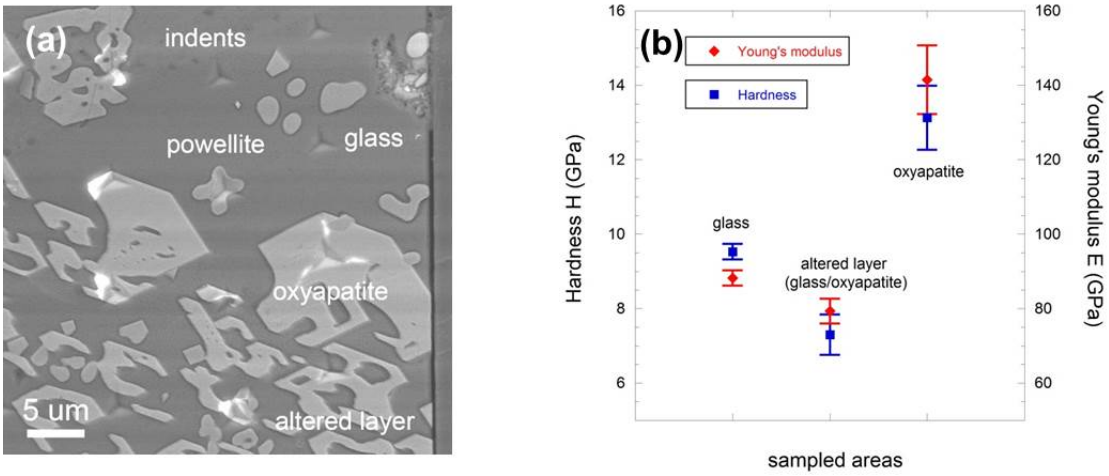

Figure 9. Mechanical properties of SPFT glass ceramic close to surface.

In Fig. 9(b), Young's modulus and hardness of glass, oxyapatite, altered layer are compared, and all these data are obtained in 10 um deep area from surface. Among these three phases, the highest modulus and hardness are found in oxyapatite, the lowest in altered layer, and glass stays in middle. In glass ceramic, it is possible to have non-durable glassy regions at the crystal-glass interface that affect the altered layer chemistry and mechanical stress as they can lead to imperfections that are selectively corroded. These mechanical properties evolutions may help us understand the corrosion behavior of glass ceramics.

2. Synchrotron Micro-X-ray Diffraction and X-ray fluorescence for multi-phase glass ceramics

Micro beam X-ray diffraction (XRD) and microfluorescence techniques were used to characterize crystal structure and elemental distribution information in multi-phase glass ceramics. Due to the complexity of multi-phase samples, it is difficult to use traditional lab

powder XRD measurement to identify individual crystalline phases in multi-phase samples. Synchrotron micro-X-ray beam provides a possibility to characterize multi-phase materials. Synchrotron X-ray beam at the 2-ID-D/E beamline in the Advanced Photon Source (APS) at Argonne National Laboratory (ANL), encompasses three hard x-ray microprobes for x-ray fluorescence mapping, fluorescence spectroscopy, and microdiffraction. The beam could be focused in a sub-micron area (0.1μm x 0.1μm) which is smaller than grain size of crystalline phases in those multi-phase glass ceramics, so we can obtain micro-XRD data similar as single crystal information and high resolution X-ray imaging.

Figure 10 shows an example of micro-XRD from a pixel material from one grain in multi-phase glass ceramic labeled "1XSC". Figure 10 (a) is the original diffraction pattern obtained from the 2-ID-D/E beamline, and (b) is the (a) pattern in θ-2θ scan. After the adjustment of energy of X-ray, this synchrotron XRD pattern is used to identify the crystalline phase. In previous study, we have successfully indexed oxyapatite ($Ca_2Nd_8Si_6O_{26}$) phase using this technique.

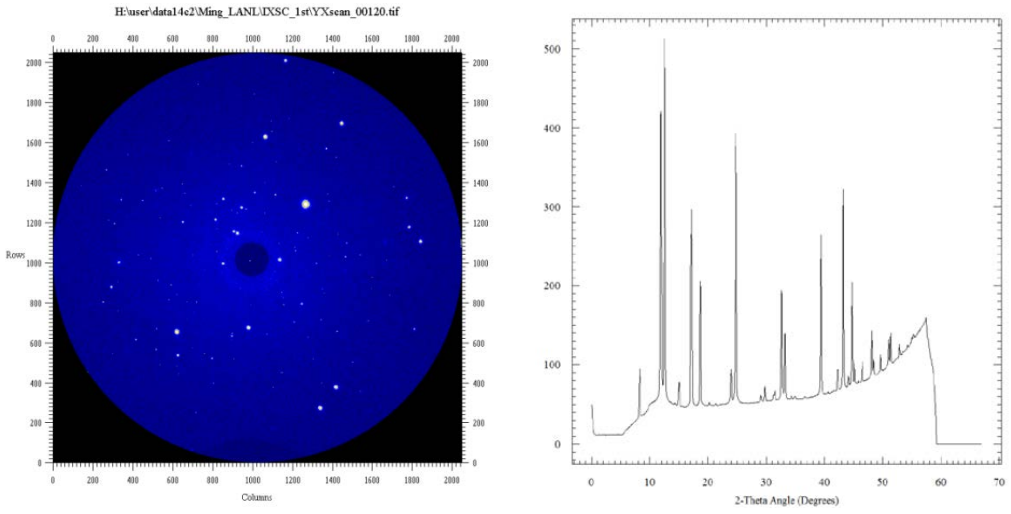

(a) (b)

Figure 10. (a) The original micro-X-ray diffraction from a pixel material of one crystal grain in multi-phase glass ceramic, (b) XRD pattern in θ-2θ scan.

Figure 11 shows an example of the elemental mapping result for multi-phase glass ceramic sample 1XSC using microfluorescence technique. This approach has successfully revealed composition structures in the differential analyses on the X-ray fluorescence images of multi-phase glass-ceramics. Figure 12 shows an example of diffraction mapping of multi-phase glass ceramic sample 1XSC at the same area of Fig. 11. Combining these two mapping information, we can get better resolution and more detail information than that of SEM/EDS. This work could demonstrate that micro-XRD and microfluorescence might be great tools to characterize multi-phase samples.

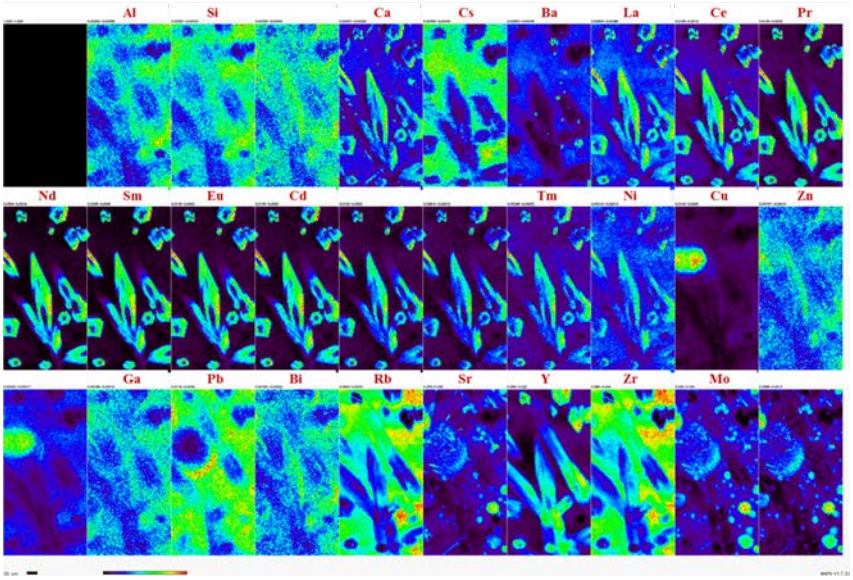

Figure 11. Microfluorescence elemental mapping of sample 1XSC.

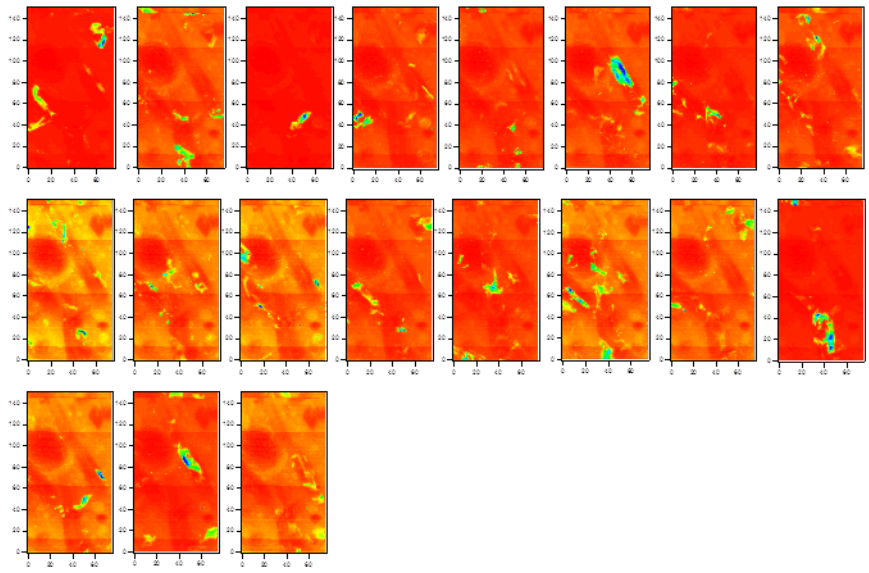

Figure 12. Diffraction mapping of sample 1XSC.

3. Future work

LANL will focus on characterization and testing procedures on glass ceramics from the test matrix and melter testing to further develop and mature the reference glass ceramic waste form. FY16 activities include: Characterize glass ceramic waste forms using various techniques including X-ray diffraction, SEM, TEM/STEM, EFTEM with EELS, nano-indentation, synchrotron X-ray, and test their corrosion behavior and radiation stability by the product consistency test, ion beam irradiation, and in-situ ion irradiation.

References

[1] G. L. McVay and L. R. Pederson, *Mat. Res. Soc. Symp. Proc.* 3, 323-330 (1980).

[2] D. E. Clark and L. L. Hench, *Nucl. Chem. Waste Mgmt.* 2, 93-101 (1981).

[3] W. Lutze, “Silicate Glasses” Chapter 1, in Radioactive Waste Forms for the Future, W. Lutze and R. C. Ewing, eds., North-Holland, New York, pp. 1-159 (1988).

[4] S. Gin, P. Jollivet, M. Fournier, F. Angeli, P. Frugier andT. Charpentier, *Nat. Commun.* 6, 6360 (2015).

[5] R. Hellmann, S. Cotte, E. Cadel, S. Malladi, L. S. Karlsson, S. Lozano-Perez, M. Cabie and A. Seyeux, *Nat. Mat.*, 14, 307-311 (2015).

[6] J. E. Mendel, Final Report of the Defense High-Level Waste Leaching Mechanism Program, Pacific Northwest Laboratory Report PNL-5157 (1984).

[7] J. C. Dran, J. C. Petit, And C. Brouse, *Nature* 319, 485-487 (1986).